Journal of Solid State Chemistry 183 (2010) 41–45

Contents lists available at ScienceDirect

Journal of Solid State Chemistry

journal homepage: www.elsevier.com/locate/jssc

Order–disorder transition in the $Nd_{2-y}Y_yZr_2O_7$ system: Probed by X-ray diffraction and Raman spectroscopy

B.P. Mandal [a], P.S.R. Krishna [b], A.K. Tyagi [a,*]

[a] Chemistry Division, Bhabha Atomic Research Centre, Mumbai 400085, India
[b] Solid State Physics Division, Bhabha Atomic Research Centre, Mumbai 400085, India

ARTICLE INFO

Article history:
Received 26 June 2009
Received in revised form
14 October 2009
Accepted 15 October 2009
Available online 22 October 2009

Keywords:
Pyrochlore
XRD
Raman spectroscopy

ABSTRACT

A series of compositions having the general formula $Nd_{2-y}Y_yZr_2O_7$ have been synthesized by heating of mixtures of oxides of the components cation and characterized by X-ray diffraction and Raman spectroscopy. Rietveld analysis on the XRD data of all the compositions has been performed which revealed a decrease in lattice parameter as a function of y in the series $Nd_{2-y}Y_yZr_2O_7$ (y=0.0–0.8). Subsequently, a biphasic region starts which continues for y=1.2 and 1.6. The other end member, i.e. $Y_2Zr_2O_7$ is found to be defect fluorite. On the other hand, Nd^{3+} has been used as surrogate material for Am^{3+}, which is a minor actinide found in spent nuclear fuel. In the pyrochlore range, the increasing trend of the x-parameter of 48f oxygen indicates the enhancement of disorder in the system. Raman spectroscopy has been employed to validate the data obtained from XRD. The involvement of 48f oxygen in disorder has also been verified by Raman spectroscopic investigation.

1. Introduction

Pyrochlore-structured compositions have been attracting an ever-growing attention due to their wide range of properties such as ionic conductivity [1,2], superconductivity [3], luminescence [4], ferromagnetism [5] and catalysis [6], etc. Moreover, the zirconate pyrochlores are important ceramic waste forms for actinide immobilization and are among the principal host phases currently considered for the disposition of Pu from dismantled nuclear weapons and reactors [7]. Pyrochlore adopts a cubic structure whose space group is $Fd\bar{3}m$, (Z=8, $a \approx 10$ Å), and the formula is ideally $^{VIII}A_2^{VI}B_2^{IV}X_6^{IV}Y$ (superscripts indicate the coordination number), where A is a mainly trivalent rare-earth ion and B cation may be transition element in their proper oxidation state [8,9]. In other words, pyrochlore is an ordered variant ($2 \times 2 \times 2$) of fluorite (AX_2) structure, except that there are two crystallographically independent cation sites and one-eighth of the anions are absent. The cell parameter of pyrochlore lattice is twice of that of fluorite lattice.

For the ordered pyrochlores, $A_2B_2O_7$, the phase stability of the superstructure is essentially determined by the radius ratio of the A and B cations. It could be mentioned here that $A_2B_2O_7$ materials with closer cationic radii are prone to crystallize as disordered fluorites instead of ordered pyrochlores. For instance, $Er_2Zr_2O_7$ having $r_A/r_B \approx 1.39$ crystallizes as a disordered fluorite structure whereas $Er_2Ti_2O_7$ with $r_A/r_B \approx 1.66$ crystallizes as an ordered pyrochlore structure [10], however, if the radius ratio is more than the stability of pyrochlore then it adopts layered monoclinic structure (e.g. $Nd_2Ti_2O_7$ etc). The pyrochlore and/or defect fluorite structure having close ionic radii of A and B cations shows exceptionally high stability in radiation environment because upon irradiation they can swap their positions to dissipate the extra energy. In view of this, $Y_2Zr_2O_7$ would be expected to be a promising host since the r_Y/r_{Zr} ratio is 1.41 which is at the borderline of pyrochlore to defect fluorite phase. On the other hand, immobilization of plutonium, americium and other minor actinides and the long lived fission products is challenging task because of their high radioactivity. In order to study the solubility of Am^{3+} in pyrochlores, Nd^{3+} can be used as surrogate material because Am^{3+} and Nd^{3+} have similar ionic radii [10] (1.02 Å in cubic coordination). Therefore, it is important to study the structure of $Y_2Zr_2O_7$ and the phase relations in the $Nd_{2-y}Y_yZr_2O_7$ series. In an attempt to explain various experimental observations of the order–disorder transitions in the pyrochlore system many groups [11–13] have calculated the defect formation energies of a large number of pyrochlore compositions. They found that the ionic size variation at B site has comparatively greater influence over the ionic size variation at A site in determining the energetics of defect formation. Lian *et al.* showed that variation in ionic size of A site ion has also enough importance on stability of pyrochlore structure [14]. Exploiting Rietveld analysis and Raman spectroscopy on the series $Y_2Ti_{2-y}Zr_yO_7$ series, Glerup et al. [15] concluded that with increase in Zr^{4+} content the system undergoes a structural transformation from the perfect pyrochlore to

* Corresponding author. Fax: +91 22 2550 5151.
E-mail address: aktyagi@barc.gov.in (A.K. Tyagi).

0022-4596/$ - see front matter © 2009 Elsevier Inc. All rights reserved.
doi:10.1016/j.jssc.2009.10.010

defect fluorite via an intermediate disordered pyrochlore phase. In this investigation, an attempt has been made to vary the composition of the *A* site cations in $Nd_{2-y}Y_yZr_2O_7$ to systematically delineate the structural evolution leading to order–disorder transitions. Raman spectroscopic technique has been employed to support the results obtained from XRD analysis.

2. Experimental details

AR grade Nd_2O_3, Y_2O_3 and ZrO_2 were first heated at 900 °C for overnight to remove moisture and other volatile impurities. Stoichiometric amounts of the reactants were weighed to get the compositions corresponding to $Nd_{2-y}Y_yZr_2O_7$. The starting reagents were mixed thoroughly and then subjected to a three step heating protocol as follows with intermittent grindings. The thoroughly ground mixtures were heated in the pellet form at 1200 °C for 36 h, followed by a second heating at 1300 °C for 36 h after regrinding and repelletizing. In order to attain a better homogeneity, the products obtained after second heating were reground, pelletized and heated at 1400 °C for 48 h, which was the final annealing temperature for all the samples. The heating and cooling rates were 2 °C per minute in every annealing steps and atmosphere was static air. The XRD pattern of samples were recorded from $2\theta = 10^\circ$ to 90° on a Philips X'pert Pro XRD unit in static air condition with monochromatized Cu$K\alpha$ radiation ($K\alpha_1 = 1.5406$ Å and $K\alpha_2 = 1.5444$ Å). The diffraction patterns were recorded in step scan mode with step width 0.02° and step time 3.30 s. The Raman spectra were recorded using a 632.8 nm line from a He–Ne laser and the scattered light was analyzed using a single stage spectrograph (Horiba JY Model HR800). The laser was focused to a spot of ~5 μm and a 10× objective lens was used for the collection of back scattered Raman signal. The instrument was calibrated before performing the measurement.

3. Results and discussions

The XRD patterns of all the products in $Nd_{2-y}Y_yZr_2O_7$ ($0.0 \le y \le 2.0$) series were recorded and analyzed. Few typical X-ray diffraction patterns are shown in Fig. 1(a–c). Structural analysis has been done by using Rietveld refinement program Fullprof-2008 [16]. In pyrochlore structure, the superstructure peaks carry some useful information about the perturbation. In present study we have analyzed the profile as well as structure factor on the basis of ordering of metal ions and displacement of oxygen ions. First of all, the background parameters were fitted. The diffraction peak profile was fitted with Pseudo-Voigt profile function and then the FWHM parameters were adjusted. No absorption parameter was considered during refinement. The *x*-parameter of 48*f* oxygen was refined for the pyrochlore samples. We have tried to refine the occupancy of oxygen ions at different sites for the single phasic samples. It has been found that with increase in Y^{3+} content in the solid solution the structure transforms from ideal pyrochlore to defect fluorite through a biphasic region. The change in lattice parameter has been listed in Table 1. The decrease in lattice parameter with increase in Y^{3+} content in the series is due to lower ionic radius of Y^{3+} (0.93 Å) compared to that of Nd^{3+} (1.02 Å) in eight fold coordination [10]. It is noticeable from the Table 1 that the lattice parameters remain unchanged for the two compositions in the region from $Nd_{0.8}Y_{1.2}Zr_2O_7$ to $Nd_{0.4}Y_{1.6}Zr_2O_7$ which confirms that these two compositions are biphasic mixture of pyrochlore and defect fluorite. During refinement it has been assumed that in $Nd_2Zr_2O_7$, the 8*a* site remains totally vacant. With increase in Y^{3+} content in the series the 8*a* site also gets populated with concomitant of depopulation of the 48*f* site. The occupancy at 8*b* site remains almost constant. The variations of oxygen occupancy were not done for the biphasic mixtures because they gave rise to

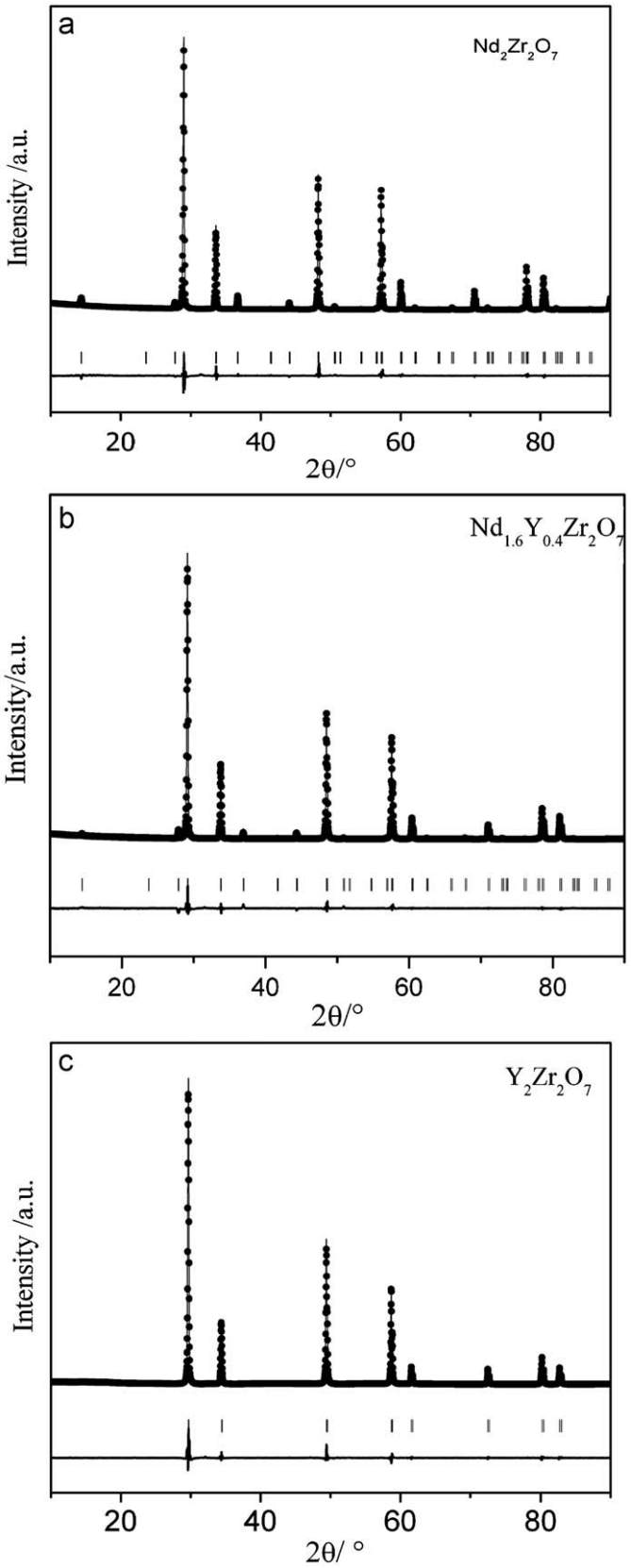

Fig. 1. Observed and calculated XRD patterns of (a) $Nd_2Zr_2O_7$, (b) $Nd_{1.6}Y_{0.4}Zr_2O_7$ and (c) $Y_2Zr_2O_7$.

Table 1
Rietveld refined parameters of $Nd_{2-y}Y_yZr_2O_7$ at different y.

	y=0.0 $Fd\bar{3}m$	y=0.4 $Fd\bar{3}m$	y=0.8 $Fd\bar{3}m$	y=1.2 (biphasic)	y=1.6 (biphasic)	y=2.0 $Fm\bar{3}m$
Lattice parameter (A)	10.666(1)	10.609(1)	10.555(2)	10.532(5)+5.218(4)	10.531(5)+5.217(5)	5.212(1)
U	0.099(4)	0.08(1)	0.0792)	0.08(9)	0.08(9)	0.083(5)
V	−0.06(4)	−0.09(4)	0.08(1)	−0.12(4)	−0.12(4)	−0.118(4)
W	0.062(1)	0.04(4)	0.04(3)	0.05(8)	0.05(8)	0.053(1)
x-parameter of 48f oxygen	0.330(1)	0.341(7)	0.345(6)	0.345(1)	0.345(3)	
Total number of independent reflections	39	39	39	39+9	39+9	9
O1 ion (48f) (x, 0.125,0.125) B (A^2)	1.9(2)	1.6(5)	1.7(4)	2.1 (5) (pyrochlore phase)	2.8 (8) (pyrochlore phase)	
O2 ion (8b) (0.125,0.125,0.125) B (A^2)	0.6(3)	1.34(3)	1.08(6)	3.1(4) (pyrochlore phase)	4.1(3) (pyrochlore phase)	
Occupation number						
48f O1	6.0	5.77(7)	5.33(8)			
8b O2	1.0	0.98(3)	0.97(4)			
8a O3	0.0	0.27(5)	0.63(5)			
R_p	7.33	6.85	7.91	7.92	8.99	6.55
R_{wp}	9.95	9.98	9.90	11.0	12.3	8.93
R_{exp}	6.41	6.11	5.96	4.5	4.21	4.68
R_B	3.39	3.60	3.52	6.12&3.74	9.12&11.7	1.40
R_F	3.09	4.69	5.96	6.57&5.99	9.88&6.29	1.19

erroneous results. The involvement of 8a oxygen and 48f oxygen in disordering also has been verified by Raman spectroscopy. Another end member, i.e. $Y_2Zr_2O_7$ crystallizes as defect fluorite structure.

Earlier it has been mentioned that $A_2B_2O_7$, A cation is surrounded by 8 oxygen ions and B cation is surrounded by 6 oxygen ions, and in fluorite type of structure all the cations gets similar kind of chemical environment. The coordination number of B site cation increases from 6 to 8 on going from pyrochlore to defect fluorite [17]. Using neutron diffraction and performing Rietveld analysis, Heremans et al. [18] studied the extent of cation antisite disorder in $Y_2(Zr_xTi_{1-x})_2O_7$ by measuring the fractional occupancy of the interstitial 8a site and the effective scattering length for the A and B-site cations. They found that with an increasing substitution of Zr, first, the 48f oxygen anions fill up the 8a vacant sites; thus suggesting that anion disorder precedes the disordering of the cation lattice. The occupancy of the interstitial 8a site increases linearly with Zr-content over the entire range of the solid solution.

Dickson et al. [19] reported that the intensity of the (111) reflection is most sensitive to the position of the x-parameter of 48f oxygen. The x-parameter of 48f oxygen moves from 0.3125 to 0.375 with increase in disorder in the system and the intensities of the characteristic pyrochlore peaks approach to zero intensity. Originally, in pyrochlore structure the oxygens are non-equivalent. The oxygen at 48f site is surrounded by two A and two B cations and 8a site is having four B neighboring atoms, and 8b site is surrounded by four A cations. However, in pyrochlore structure, the 8a position is vacant, therefore, the 48f oxygen shifts from its ideal tetrahedral position towards two of its B cations to compensate the charge over B cations. Rietveld analysis reveals that with increase in the Y^{3+} content in titled series, the shift of 48f oxygen towards B cation decreases leading to increase in the x-parameter of 48f oxygen (keeping B cation at origin) which drives the system to transform from ordered pyrochlore to defect fluorite. In a perfect pyrochlore structure ($A_2B_2O_6O'$), the 48f oxygen's x-parameter lies within the limit 0.3125–0.375 taking origin (0,0,0) at the B cation site [1,20]. At x=0.3125, the B ion has a perfect octahedral coordination and 'A' cation resides at the center of distorted hexagonal (six 48f O) network with two oxygens (8b O′) perpendicular to the hexagonal plane [20,21]. Again, with variation in x-parameter the shape of polyhedra in pyrochlore also changes. Based on Madelung energy and site potential calculations, it had been found that (3+, 4+) pyrochlores with $x \approx 0.36$ may also exist but in a highly disordered state [22,23]. Earlier we [24] have shown that for $Dy_2Hf_2O_7$, the x-parameter is 0.348 and it crystallizes as a disordered pyrochlore. In our present investigation, we observed that the x-parameter ranges from 0.330(1) for $Nd_2Zr_2O_7$ to 0.345(6) for $Nd_{0.8}Y_{1.2}Zr_2O_7$, then it becomes constant since another phase evolution starts from that composition (y=1.2) onwards. Other end member, i.e. $Y_2Zr_2O_7$ (or $Y_{0.5}Zr_{0.5}O_{1.75}$) is found to be defect fluorite.

Earlier Moringa et al. [25] also reported that in $Zr_{0.786}Y_{0.214}O_{1.893}$ system that few percent of O atoms displaced from its ideal position. Ishizawa et al. [26] found in $Zr_{0.758}Y_{0.242}O_{1.879}$ system that the structure is defect fluorite but the Zr and O atoms are shifted slightly from their ideal positions. In this manuscript also, an attempt has been made to investigate the structure of $Y_2Zr_2O_7$ following the work of Moringa et al. and Ishizawa et al.

3.1. Ideal defect fluorite model

In this model it has been proposed that the cations are at 4a site, i.e. (0,0,0) site and the oxygen atoms occupy the 8c site (0.25,0.25,0.25), following symmetry of $Fm\bar{3}m$ space group. The final residual factors are found to be R_B=1.4, R_F=1.19, R_p=6.55, R_{wp}=8.98 based on ideal fluorite structure. In $Zr_{0.786}Y_{0.214}O_{1.893}$ system, it has found that few percent of O atoms displaced by 0.26 Å along $<100>$ direction from its ideal position while remaining O-atoms reside at the ideal positions of fluorite-type structure. These observations inspired us to assume that in $Y_{0.5}Zr_{0.5}O_{1.75}$ may also have some deviations from ideal fluorite model.

3.2. Cations (Y^{3+}, Zr^{4+}) shift model

In this model it has been assumed that few percent of the oxygen atom (O2) occupy the 48 g site (x, 0.25, 0.255) and the rest of the oxygen atoms (O1) occupied 8c site (0.25, 0.25, 0.25). On the other hand, the cations can occupy 32f site (x,x,x), in addition to standard 4a (0,0,0) site of perfect fluorite structure. All the positional parameters were refined and the coordinates for O2 were found to be (0.339(4), 0.25, 0.25) and the 32f's positional coordinate is found to be (0.016(1), 0.016(1), 0.016(1)). Initially, it

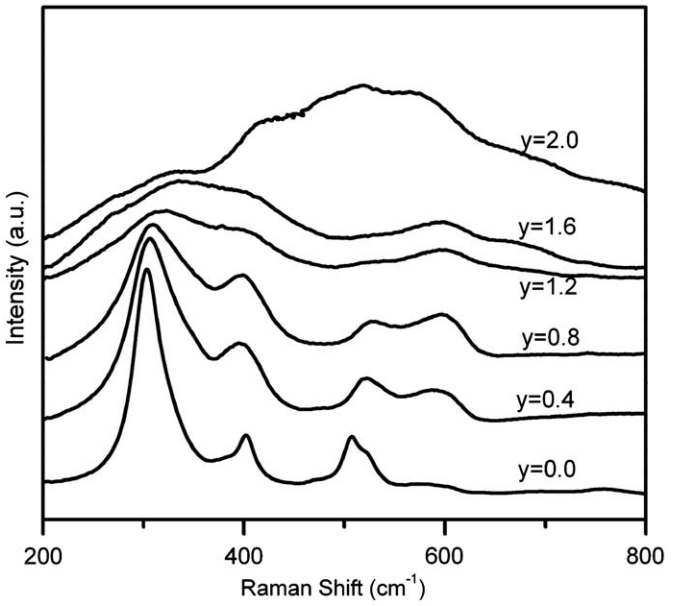

Fig. 2. Raman spectra of $Nd_{2-y}Y_yZr_2O_7$ with increasing concentration of Y^{3+}: (a) $Nd_2Zr_2O_7$, (b) $Nd_{1.6}Y_{0.4}Zr_2O_7$, (c) $Nd_{1.2}Y_{0.8}Zr_2O_7$, (d) $Nd_{0.8}Y_{1.2}Zr_2O_7$, (e) $Nd_{0.4}Y_{1.6}Zr_2O_7$ and (f) $Y_2Zr_2O_7$.

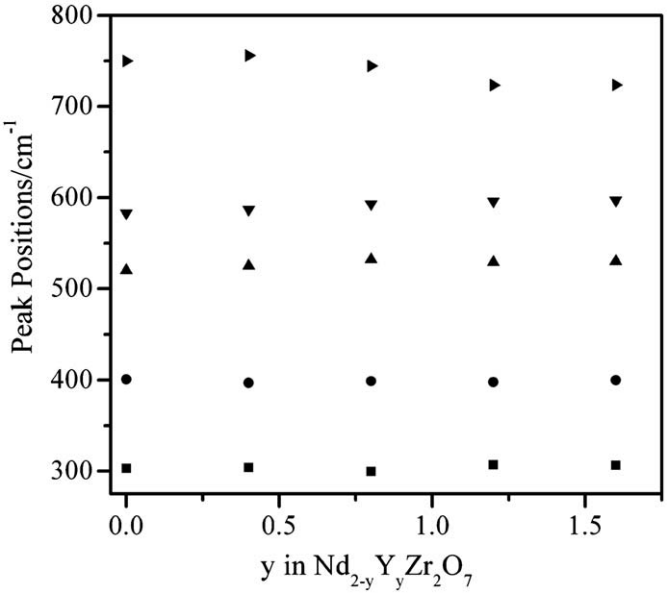

Fig. 3. Change in the frequency of different modes with increasing concentrations of Y^{3+} in $Nd_{2-y}Y_yZr_2O_7$ series.

Table 2
Raman mode frequencies with symmetry character and vibration types.

Frequency (cm^{-1})	Symmetry	Vibration mode
302	E_g	B–O_6 bending
400	T_{2g}	Mostly B–O strech with mixture of A–O strech and O–B–O bending vibrations
507	T_{2g}	Mostly O–B–O bend with mixture of B–O and B–O stretch
520	A_{1g}	Mostly O–B–O bending
585	T_{2g}	Mostly B–O stretching
750	T_{2g}	Mostly B–O stretching

was assumed that Y^{3+} and Zr^{4+} have taken 32*f* and 4*a* sites, respectively, but the resultant residual *R* factors were not satisfactory. Vice versa has also been tried which also not lead to convincing results. Finally, it was assumed that both the sites (4*a* and 32*f*) are occupied by both Y^{3+} and Zr^{4+} then also the refinement does not result to meaningful R-parameters.

So it can again be stated that ideal fluorite model may be the correct model for $Y_2Zr_2O_7$ structure.

4. Raman spectroscopy

X-ray diffraction studies are more sensitive to disorder in the cationic sublattice in comparison with anionic sublattice whereas Raman spectroscopy is essentially sensitive to oxygen-cation vibrations and is an excellent tool to determine the local disorder. The Raman spectroscopic studies have been found to provide explicit information [15] to distinguish between a pyrochlore, biphasic mixture and a defect-fluorite material. Therefore, all the compounds in the present investigation were further investigated by Raman spectroscopy over the frequency range 200–800 cm^{-1} to investigate the composition at and beyond which pyrochlore lattice undergoes a transformation to disordered pyrochlore. Cubic pyrochlore, $A_2B_2O_7$, belongs to space group ($Fd\bar{3}m$, O_h^7) with $Z=8$ has six Raman active modes and seven IR active mode for the vibration spectroscopy which can be represented as [27–29]

$$\Gamma = A_{1g} + E_g + 4T_{2g} + 7T_{1u}$$

Among these modes, the Raman active modes are $A_{1g}+E_g+4T_{2g}$. On the other hand, cubic fluorite belongs to the space group ($Fm\bar{3}m$, O_h^5) with $Z=4$ which has only one Raman active mode ($\Gamma=T_{2g}$) [30]. All the six modes of pyrochlores have been found in the Raman spectra which are shown in Fig. 2. The Raman peaks have been assigned by following Vandenbore's work on pyrochlores [27] (Table 2). Only difference is that they had observed two separate modes at 523 and 532 cm^{-1}, whereas we observe a broad peak, which could be resolved into two components at 507 and 520 cm^{-1} using least square fitting with two lorentzians. According to the polarized Raman measurement presented in literature [27,31] the peak at 520 cm^{-1} is assigned to A_{1g} mode since its intensity changes significantly with different directions of polarization. The other bands, at around 400, 507, 585 and 750 cm^{-1}, are due to T_{2g} modes of the pyrochlore structure. The band at 302 cm^{-1} has been assigned to E_g mode following our earlier work [20]. All the Raman peaks of all the samples except pure $Nd_2Zr_2O_7$ are quite broad. This broadening is not attributed to the smaller particle size because the samples were synthesized by ceramic sintering route and the XRD patterns are reasonably sharp which indicates the size of the particles are in micro regime. Ordered compounds like pyrochlore, also have disorder due to presence of vacancy and defects and foreign ions which disrupts the translational symmetry in the lattice and consequently it relaxes the $k \approx 0$ selection rule. Hence, phonons from all parts of the Brillouin zone start contributing to the optical spectra, thereby giving rise to broadened, continuously spread, and weak-intensity bands [20]. The intensity of the peak at 304 cm^{-1} get diminished with increase in Y^{3+} content in the compositions and it becomes broad band from $y=1.2$ onwards. The qualitative nature of the Raman bands remain similar till $Nd_{1.2}Y_{0.8}Zr_2O_7$, afterward the spectra show huge broadening for the samples $y=1.2$ and 1.6. The Raman spectra of another end member, i.e. $Y_2Zr_2O_7$, which has been found as disordered fluorite by XRD, is also too broad. It is reported that for $Y_2Hf_2O_7$, $Ho_2Hf_2O_7$, $Er_2Hf_2O_7$ where the r_A/r_B ratio of compounds are more close to

defect fluorite (close to r_A/r_B ratio of $Y_2Zr_2O_7$) shows similar type of Raman spectra [24] and it has been argued that huge disorder in the compound causes the broadening.

In Fig. 2, it has been found that the intensity of the peak at $\approx 520\,cm^{-1}$ decreases whereas that of the peak at $585\,cm^{-1}$ increases in the series as a function of Y^{3+} content within the single phasic region. As the content of Y^{3+} increases, the two nearby modes at 507 and $520\,cm^{-1}$ become extremely broad and could not be resolved into two separate modes and subsequently merge with each other and their intensity in $Nd_{0.8}Y_{1.2}Zr_2O_7$ and $Nd_{0.4}Y_{1.6}Zr_2O_7$ become negligible. The changes in frequencies of different modes with change in compositions have been shown in Fig. 3. It can be clearly inferred from Fig. 3 that there is very little change in the peak positions with compositions which is probably due to sole involvement of oxygen ion movement, not Nd^{3+} or Y^{3+} ion. The striking observation is that the intensity of the strong characteristic pyrochlore Raman mode at $\approx 302\,cm^{-1}$ (E_g) steadily diminishes (see Fig. 2) and there is considerable broadening of the mode, whereas the intensity of mode at $400\,cm^{-1}$ (T_{2g}) remains almost unchanged. Factor group analysis [32,33] shows that 8*b* oxygen is involved in one of the T_{2g} mode and other three T_{2g} modes are related to 48*f* oxygens. This signifies the fact that 8*b* site oxygen is related with the T_{2g} mode which appears at $400\,cm^{-1}$. It has been argued that Raman lines are broadened due to structural disorder or lattice strain [28,32]. So with increase in amount of Y^{3+} in the solid solution, the weakening of intensity of $302\,cm^{-1}$ band (which is related with 48*f* oxygen) means the disorder is associated with 48*f* oxygen site. The almost unchanged intensity of the $400\,cm^{-1}$ band, which is related to one of 8*b* oxygen, suggests that the 8*b* oxygen site remain almost undisturbed with change in Y^{3+} content in the series. Qu et al. [30] also found similar kind of result in MgO doped $Sm_2Zr_2O_7$ samples.

The Raman spectra of samples with $y=1.2$ and 1.6 (Fig. 2) exhibit signature of both defect fluorite and pyrochlore, suggesting the compositions is a biphasic mixture, which corroborate our XRD analysis.

5. Conclusions

A series of compounds with the nominal compositions $Nd_{2-y}Y_yZr_2O_7$ ($0.0 \le y \le 2.0$) were prepared by solid state route. The continuous decrease in the lattice parameter with increase in Y^{3+} content till $y=0.8$ in the series proves the homogeneity range till that compositions. With increase in Y^{3+} content in the system, the distinction between A and B sites diminishes which further leads to antisite defects formation which results into local oxygen disorder as evidenced by increased width of the Raman modes. The next two compositions, i.e. $y=1.2$ and 1.6 are found to be biphasic in nature. The *x* parameter of 48*f* oxygen of compositions with pyrochlore structure shifts from 0.330(1) for $Nd_2Zr_2O_7$ to 0.345(6) for $Nd_{0.8}Y_{1.2}Zr_2O_7$, which is clear indication of increase in disorder in the system. One more significant conclusion can be drawn that variation at A site can also leads to order–disorder transition which supports the theoretical predication of Lian et al. [14]. Interestingly, Raman spectroscopy substantiated the result obtained from XRD data analysis. All the Raman peaks could be assigned properly. Moreover, this study revealed that 48*f* oxygen is involved in anionic disorder.

Acknowledgments

Authors are thankful to Ms. A. Banerji and Ms. Meenakshi for recording Raman Spectra.

Appendix A. Supplementary material

Supplementary data associated with this article can be found in the online version at doi:10.1016/j.jssc.2009.10.010.

References

[1] B.J. Wuensch, K.W. Eberman, C. Heremans, E.M. Ku, P. Onnerud, E.M.E. Yeo, S.M. Haile, J.K. Stalick, J.D. Jorgensen, Solid State Ionics 129 (2000) 111.
[2] B.P. Mandal, S.K. Deshpande, A.K. Tyagi, J. Mater. Res. 23 (2008) 911.
[3] J. Yamaura, Y. Muraoka, F. Sakai, Z. Hiroi, J. Phys. Chem. Solids 63 (2002) 1027.
[4] J.K. Park, C.H. Kim, K.J. Choi, H.D. Park, S.Y. Choi, J. Mater. Res. 16 (2001) 2568.
[5] M.J.P. Gingras, B.C. den Hertog, M. Faucher, J.S. Gardner, S.R. Dunsiger, L.J. Chang, B.D. Gaulin, N.P. Raju, J.E. Greedan, Phys. Rev. B 62 (2000) 6496.
[6] J.M. Sohn, S.I. Woo, Catal. Lett. 79 (2002) 45.
[7] R.C. Ewing, W.J. Weber, J. Lian, J. Appl. Phys. 95 (2004) 5949.
[8] M.A. Subramanian, G. Aravamudan, G.V. Subba Rao, Prog. Solid State Chem. 15 (1983) 55.
[9] W.R. Panero, L. Stixrude, R.C. Ewing, Phys. Rev. B 70 (2004) 054110.
[10] R.D. Shanon, Acta Crystallogr. A 32 (1976) 751.
[11] M. Pirzada, R.W. Grimes, L. Minervini, J.F. Maguire, K.E. Sickafus, Solid State Ionics 140 (2001) 201.
[12] K.E. Sickafus, L. Minervini, R.W. Grimes, J.A. Valdez, M. Ishimaru, F. Li, K.J. McClellan, T. Hartmann, Science 289 (2000) 748.
[13] P.J. Wilde, C.R.A. Catlow, Solid State Ionics 112 (1998) 173.
[14] J. Lian, J. Chen, L.M. Wang, R.C. Ewing, J.M. Farmer, L.A. Boatner, K.B. Helean, Phys. Rev. B 68 (2003) 134107.
[15] M. Glerup, O.F. Nielsen, F.W. Poulsen, J. Solid State Chem. 160 (2001) 25.
[16] WinPLOTR, J Rodríguez-Carvajal, Laboratorie Leon Brillouin (CEA-CNRS) April 2005 (LLB-LCSIM).
[17] P. Nachimuthu, A. Thevuthasan, E.M. Adams, W.J. Weber, B.D. Begg, B.S. Mun, D.K. Shuh, D.W. Lindle, E.M. Gullikson, R.C.C. Perera, J. Phys. Chem. B Lett. 109 (2005) 1337.
[18] C. Heremans, B.J. Wuensch, J.K. Stalick, E. Prince, J. Solid State Chem. 117 (1995) 108.
[19] S.J. Dickson, K.D. Hawkings, T.J. White, J. Solid State Chem. 82 (1986) 146.
[20] B.P. Mandal, A. Banerji, V. Sathe, S.K. Deb, A.K. Tyagi, J. Solid State Chem. 180 (2007) 2643.
[21] H.S. Horowitz, J.M. Longo, J.T. Lewandowski, Mater. Res. Bull. 16 (1981) 489.
[22] J. Pannetier, J. Phys. Chem. Solids 34 (1973) 583.
[23] W.W. Barker, P.S. White, O'. Knop, Can. J. Chem. 54 (1976) 2316.
[24] B.P. Mandal, N. Garg, S.M. Sharma, A.K. Tyagi, J. Solid State Chem. 179 (2006) 1999.
[25] M. Moringa, J.B. Cohen, J. Faber, Acta Cryst. A 35 (1979) 789.
[26] N. Ishizawa, Y. Matshuhima, M. Hayashi, M. Ueki, Acta. Cryst. B 55 (1999) 726.
[27] M.T. Vandenborre, E. Husson, J.P. Chatry, D. Michel, J. Raman Spectrosc. 14 (1983) 63.
[28] H.C. Gupta, S. Brown, N. Rani, V.B. Gohel, J. Raman Spectrosc. 32 (2001) 41.
[29] N. Garg, K.K. Pandey, C. Murli, K.V. Shanavas, B.P. Mandal, A.K. Tyagi, S.M. Sharma, Phys. Rev. B 77 (2008) 214105.
[30] N. Kjerulf-Jensen, R.W. Berg, F.W. Poulsen, in: Thorstensen (Ed.), Proceedings of the Second Europian Solid Oxide Fuel Cell Forum, vol. 2, Norway, 1996, p. 647.
[31] Z. Qu, C. Wan, W. Pan, Chem. Mater. 19 (2007) 4913.
[32] B.E. Scheetz, W.B. White, J. Am. Ceram. Soc. 62 (1979) 468.
[33] D. Michel, M.J. Perez, R. Collongues, Mater. Res. Bull. 9 (1974) 1457.